SERI/TP-214-2563
UC Category: 60
DE85000530

A Computer Analysis of Wind Turbine Blade Dynamic Loads

Robert Thresher
Edward L. Hershberg
Alan D. Wright

November 1984

To be presented at the 1985
ASME Wind Symposium IV
Dallas, Texas
18-20 February 1985

Prepared under Task No. 4820.10
FTP No. 478

Solar Energy Research Institute
A Division of Midwest Research Institute

1617 Cole Boulevard
Golden, Colorado 80401

Prepared for the
U.S. Department of Energy
Contract No. DE-AC02-83CH10093

Printed in the United States of America
Available from:
National Technical Information Service
U.S. Department of Commerce
5285 Port Royal Road
Springfield, VA 22161
Price:
Microfiche A01
Printed Copy A02

A COMPUTER ANALYSIS OF WIND TURBINE BLADE DYNAMIC LOADS

Robert W. Thresher
Alan D. Wright

Solar Energy Research Institute
Wind Energy Research Center
1617 Cole Blvd.
Golden, CO 80401

Edward L. Hershberg

Techtronics Incorporated
Beaverton, OR 97302

ABSTRACT

The flapping motion of a single wind turbine rotor blade has been analyzed and equations describing the flapping motion have been developed. The analysis was constrained to allow only flapping motions for a cantilevered blade, and the equations of motion are linearized.

A computer code, called FLAP (Force and Loads Analysis Program), to solve the equations of motion and compute the blade loads has been completed and compared to measured loads for a 3-bladed downwind turbine with stiff blades. The results of the program are presented in tabulated form for equidistant points along the blade and equal azimuth angles around the rotor disk. The blade deflection, slope and velocity, flapwise shear and moment, edgewise shear and moment, blade tension, and blade torsion are given. The deterministic excitations considered in the analysis include wind shear, tower shadow, gravity, and a prescribed yaw motion.

INTRODUCTION

The objectives of the research described in this paper were threefold:

1. Development of an analytical model for the flapping response and dynamic loads experienced by a wind turbine rotor blade.
2. Development of an interactive, user-friendly computer code written in FORTRAN V and available in the public domain for computing the response and loads.
3. Verification of the model and the computer code with available machine data.

The model allows only flapping motion of an individual wind turbine blade. It accounts for the blade bending deformation about the smallest blade inertia axis. The rotor is assumed to rotate at a constant speed, but the hub is allowed to move in a prescribed yawing motion. Rotors that are tilted and yawed relative to the mean wind direction can be accommodated in a straightforward manner.

The model and the code are designed to operate with aerodynamic models of varying sophistication. Currently the model is configured to include the effects due to the mean wind, wind shear, and tower shadow. The code is structured in such a manner that time-dependent turbulent wind fluctuations can be added in the future. The rotor blade flapping motion is represented by a set of coordinate shape functions that are simple polynomials. Four functions are included in the computer code, but any number of the functions can be used, from only one up to the maximum of four. At present only cantilever blade attachment conditions have been implemented in the code. Thus, for the results presented in this report, the flapping motion is represented with only one coordinate function (i.e., one flap degree of freedom).

The current version for the aerodynamic model uses a quasi-steady linear aerodynamic model to compute the blade aerodynamic forces. However, the code has been designed to use more sophisticated aerodynamic force models, including time-dependent aerodynamics such as those involved in dynamic stall computations.

The model operates in the time domain, and the blade acceleration equation is integrated via a modified Euler trapezoidal predictor-corrector method. The method involves the use of a set of low order relations, is self-starting and stable, and allows frequent step size changes. The procedure is entirely automated within the computer program. Results of the blade loads analysis are printed in tabular form, and include the deflection, slope, and velocity, the flapwise shear and moment, edgewise shear and moment, blade tension, and blade twisting moment for any point along the blade axis.

The program, written in FORTRAN V, is in the public domain and was developed for easy end-user modification and customization. A substantial effort has been made to make the actual code contain its own

documentation through extensive use of comments within the program.

STRUCTURAL EQUATIONS

Moment Curvature Relationship

The blade is assumed to be a long slender beam so that the normal strength of materials assumptions concerning the bending deformation are valid. Figure 1 shows an infinitesimal element of the deformed blade. It is assumed that the blade bends only about its weakest principal axis of inertia; in the figure this is the x_p axis. No other deformations are considered.

The strength of materials bending analysis assumes a one-dimensional form for Hooke's Law that neglects all stresses except the longitudinal bending stress. It results in the following moment curvature relationship:

$$M_{x_p} = - EI_{x_p} \frac{d^2 v}{dz_p^2} , \qquad (1)$$

where M_{x_p} is the bending moment about the blade principal axis of inertia x_p, E is the elastic modulus, I_{x_p} is the area moment of inertia about the x_p axis, and v is the bending displacement in the y_p direction.

Equilibrium Equations

The equations of equilibrium are derived by summing forces and moments in the three coordinate directions. Referring to Figure 1, p_{x_p}, p_{y_p} and p_{z_p} are the applied forces per unit length and q_{x_p}, q_{y_p}, and q_{z_p} are the applied moments per unit length. The p's and q's are the sum of all applied loadings, both aerodynamic and inertial. The internal bending moments in the blade are M_{x_p}, M_{y_p}, and M_{z_p}, and the internal forces are V_{x_p}, V_{y_p}, and T. Summing forces and moments gives:

x direction: $V'_{x_p} + p_{x_p} = 0$ (2a)

y direction: $V'_{y_p} + p_{y_p} = 0$ (2b)

z direction: $T' + p_{z_p} = 0$ (2c)

x direction: $M'_{x_p} - V_{y_p} + Tv' + q_{x_p} = 0$ (3a)

y direction: $M'_{y_p} + V_{x_p} + q_{y_p} = 0$ (3b)

z direction: $M'_{z_p} - V_{x_p} v' + q_{z_p} = 0$ (3c)

where the symbol (') implies the operation $\frac{d}{dz_p}$.

Differentiation of the moment Eqs. 3a and 3b allows substitution of Eqs. 2a and 2b to eliminate the shearing forces V_{x_p} and V_{y_p}. In addition the y moment equation can be used to eliminate the shear force V_{x_p} in the z moment equation. Finally, the moment curvature relationship can be used to replace M_x in the x direction moment equations. These substitutions give the following combined equilibrium equations:

Flap: $(-v'' EI_{y_p})'' + (Tv')' + q'_{x_p} + p_{y_p} = 0$ (4a)

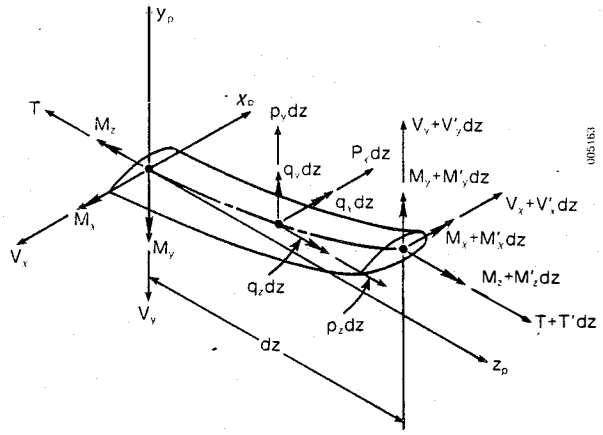

Figure 1. Blade element showing forces and moments, all acting in a positive sense.

Lead-Lag: $M_{y_p} + q'_{y_p} - p_{x_p} = 0$ (4b)

Torsion: $M'_{z_p} + M'_{y_p} v' + q_{y_p} v' + q_{z_p} = 0$ (4c)

Tension: $T' + p_{z_p} = 0$ (4d)

Coordinate System Definitions

Figure 2 shows the orientation of the turbine blade under analysis with all the intermediate coordinates required to represent the blade motion. The capital X,Y,Z coordinates are the fixed reference system. The mean wind velocity at the hub, V_{hub}, and its fluctuating components, δV_X, δV_Y, and δV_Z, are given in this system. The rotor spin axis is allowed to tilt through a fixed angle χ and the rotor is allowed to have a prescribed time-dependent yawing motion given as $\phi(t)$, where ϕ is the yaw angle. The yaw axis is coincident with the Z coordinate axis. The hub, located a distance "a" from the yaw axis, is considered to be rigid and to have some radius h. The flexible portion of the blade begins at the outer hub radius, h. The airfoil shape may begin at h or at some position further out along the blade z axis. The blade is coned at some angle β_o as shown in the figure.

The x,y,z coordinates are located in the surface of revolution that a rigid blade would trace in space, with the y axis normal to this surface. The x_p,y_p,z_p are the blade principal bending coordinates, where the z_p axis is coincident with the elastic axis of the undeformed blade. Bending takes place about the x_p coordinate. It is further assumed that the blade principal axes of area inertia do not change along the z_p axis. The influence of blade twist on bending displacement is neglected. The orientation used to set the angle θ_p for computations is the principal axis near the blade tip, because the deformation is largest there. The final coordinate system is the η,ζ,ξ system which is on the principal axes of the deformed blade at some point along the elastic axis.

The coordinate transformation which takes vector components from the fixed X,Y,Z system to the blade undeformed principal coordinates x_p,y_p,z_p is given by

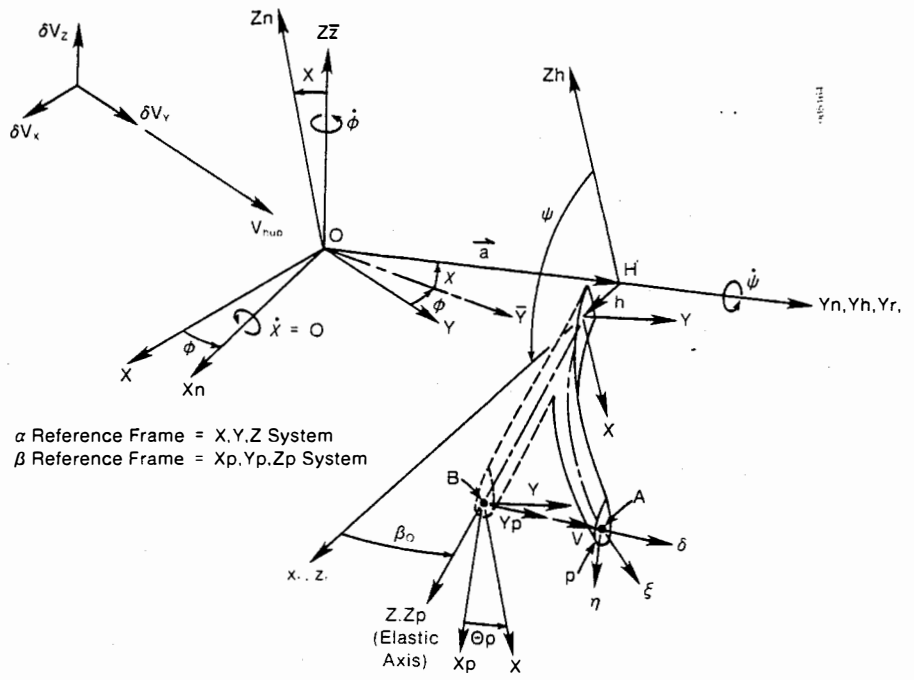

Figure 2. Illustration of the rotor system coordinates with positive displacements and rotations shown.

$$\begin{Bmatrix} x_p \\ y_p \\ z_p \end{Bmatrix} = \begin{bmatrix} (c\theta_p c\psi + \beta_o s\theta_p s\psi + \phi s\theta_p) & (c\theta_p c\psi\phi - s\theta_p + \chi c\theta_p s\psi) & (-\chi s\theta_p - c\theta_p s\psi + \beta_o s\theta_p c\psi) \\ (s\theta_p c\psi - \beta_o c\theta_p s\psi - \phi c\theta_p) & (s\theta_p c\psi\phi + c\theta_p + \chi s\theta_p s\psi) & (\chi c\theta_p - s\theta_p s\psi - \beta_o c\theta_p c\psi) \\ s\psi & (\phi s\psi + \beta_o - \chi c\psi) & c\psi \end{bmatrix} \begin{Bmatrix} X \\ Y \\ Z \end{Bmatrix} \quad (5)$$

where this transformation has been linearized for small yaw angles ϕ, small tilt, χ, and small coning angles β_o. The angle of the principal axis θ_p has been assumed to be large. The azimuth angle ψ is, of course, considered to be large. In addition, shorthand expressions for sin θp and cos θp have been written $s\theta p$ and $c\theta p$, and similar shorthand is used for sin ψ and cos ψ. The inverse transformation taking the x_p, y_p, z_p components into the X,Y,Z system is given by the transpose of the above matrix. Notice that the ψ = 0 position is with the rotor straight up at the 12 o'clock position and that Figure 2 has been drawn for the special case of $\psi = 90^o$ for convenience. The necessary intermediate coordinate transformations for components in other coordinates can be obtained as follows:

1. Set θ_p = 0 for transforming to the x,y,z,system.
2. Set θ_p = 0 and β_o = 0 for transforming to the x_r, y_r, z_r system.
3. Set θ_p = 0, β_o = 0, and ψ = 0 for transforming to the x_h, y_h, z_h system.

One additional transformation is necessary to obtain components in the deformed blade system. For small deformations this is

$$\begin{Bmatrix} \eta \\ \zeta \\ \xi \end{Bmatrix} \quad \begin{bmatrix} 1 & 0 & 0 \\ 0 & 1 & -v' \\ 0 & v' & 1 \end{bmatrix} \quad \begin{Bmatrix} x_p \\ y_p \\ z_p \end{Bmatrix} \quad (6)$$

WIND INPUTS

Wind Shear Velocity Distribution

The change in mean velocity with height above the ground is often described by the simple power law as

$$V(H) = V(H_o)\left(\frac{H}{H_o}\right)^m , \quad (7)$$

where H is the height above ground, H_o is the reference height, and $V(H_o)$ is the reference velocity at height H_o. The exponent m is called the shear exponent. For a wind turbine it is convenient to let H_o = hub height and $V(H_o) = V_h$ = hub height wind velocity. The wind may be described in the rotor hub coordinates x_h, y_h and z_h, or in terms of the blade coordinates x_p, y_p, z_p by letting $z_h = r\cos\psi$ and $r = (h+z_p)$, and expanding in powers of (z_h/H_o) and harmonics of the azimuth angle ψ to obtain

$$V(z) = V_h\left\{1 + \left(\frac{z_h}{H_o}\right)\right\}^m = V_h\{1 + W_s(r,\psi)\} , \quad (8)$$

where the wind shear coefficient W_s is

$$W_s(r,\psi) = \frac{m(m-1)}{4}\left(\frac{r}{H_o}\right)^2 + m\left(\frac{r}{H_o}\right)\cos\psi + \frac{m(m-1)}{4}\left(\frac{r}{H_o}\right)^2 \cos 2\psi . \quad (9)$$

In this expression, the harmonics above cos2ψ have been neglected.

Wind Velocity in the Tower Shadow

The shadow region behind the tower has been assumed to have a velocity profile of the form

$$V(z,\psi) = V(z)\{1 - T_s(\psi)\} , \qquad (10)$$

where

$$T_s(\psi) = \begin{cases} t_o + t_p \cos\{p(\psi-\psi_s)\} \text{ for } \psi_s - \psi_o \le \psi \le \psi_s + \psi_o \\ 0 \text{ elsewhere} \end{cases} \qquad (11)$$

and $p = 2\pi k/2\Psi_o$ is an integer.

The parameters t_o, t_p, ψ_o, ψ_s, and k are selected to give the desired approximation for the velocity profile in a pie-shaped region of $2\psi_o$. The deficit is often modeled as a $\sin^2$ function. This can be accomplished by setting: $t_o = t_p = \Delta V/2$ "one-half of desired velocity deficit"; ψ_o = "shadow half angle"; ψ_s = "shadow position," usually 180° degrees; k = "number of oscillations" (1 for this case). This shadow profile is reasonably general and many other shapes are possible. For example, a three legged tower with a peak deficit of ΔV could be modeled by setting: $t_o = t_p = \Delta V/2$ and k = 3. This would give a velocity profile with three peaks in the tower shadow region.

Combined Wind Effects

The combined effect of both wind shear and tower shadow can be written as

$$V_w(r,\psi) = V_h \{1 + W_s(r,\psi)\} \{1 - T_s(\psi)\}$$

$$V_w(r,\psi) \simeq V_h\{1 + W_s(r,\psi) - T_s(\psi)\} , \qquad (12)$$

where the combined effect has been linearized by dropping the product term $T_s(\psi)\, W_s(r,\psi)$.

The net wind velocity is specified in the X,Y,Z coordinate system and is composed of steady terms and turbulence inputs as follows:

$$\vec{V}_{wind} = R\Omega \underbrace{\begin{Bmatrix} 0 \\ \overline{V}_r + \delta\overline{V}_r \\ 0 \end{Bmatrix}_{X,Y,Z}}_{\text{Steady}} + R\Omega \underbrace{\begin{Bmatrix} \delta\overline{V}_x \\ \delta\overline{V}_y \\ \delta\overline{V}_z \end{Bmatrix}_{X,Y,Z}}_{\text{Turbulence}} \qquad (13)$$

The turbulence inputs are not specifically defined in this paper but provision is made for them to be considered at a later date. The variables in this expression are defined as follows:

- V_r = Hub velocity minus induced velocity due to uniform inflow
- $\overline{V}_r = V_h/R\Omega - v_o(r)/R\Omega$
- V_h = Hub height mean wind velocity
- $\delta\overline{V}_r$ = Variation in rotor disk velocity minus associated induced flow
- $\overline{\delta V_r} = V_h W_s(r,\psi)/R\Omega - V_h T_s(r,\psi)/R\Omega - \delta v_i(r,\psi)/R\Omega$
- W_s = Wind shear coefficient
- T_s = Tower shadow coefficient
- δv_i = Steady induced flow associated with the effects of wind shear and tower shadow
- $\delta\overline{V}_x$ = $\delta V_x/R\Omega$, $\delta\overline{V}_y = \delta V_y/R\Omega$, and $\delta\overline{V}_z = \delta V_z/R\Omega$ are the wind fluctuations associated with turbulence and no induced flows computed.

Although the analysis of this section has made provisions for wind turbulence excitations to be included as wind input, no specific recommendations can be made at this time. It seems clear from recent field studies of experimental turbines that wind turbulence plays an important part in the excitation input. No validated approaches for simulating this input are yet available.

For this analysis it is assumed that the induced velocity can be written in the form

$$v_i(r,\psi) = v_o(r) + \delta v_i(r,\psi)$$

$$v_i(r,\psi) = v_o(r) + \sum_{n=1}^{N} \{v_{nc}(r)\cos n\psi + v_{ns}(r)\sin n\psi\} - v_p\cos\{p(\psi - \psi_s)\} , \qquad (14)$$

where the $v_o(r)$ term is associated with the mean wind V_h, the v_{nc} and v_{ns} terms are associated with the nonuniform contributions caused by wind shear and yaw misalignment, and the v_p term is due to the tower shadow.

The magnitude of each of these various induced flow contributions is estimated using a simple balance of momentum at the turbine rotor. This is done for the special case of a linear relationship between the lift coefficient and the angle of attack. It results in a closed-form solution which includes the effect of wind shear, yaw orientation, and tower shadow. The reader interested in the procedure used for computation of the induced flows is referred to reference (1).

KINEMATICS

Velocity Analysis

Referring to Figure 2, designate the X,Y,Z ground-based coordinates as the α reference frame. Call the x_p,y_p,z_p principal coordinates, located at point B, the β reference frame. The velocity for an arbitrary point A on the deformed blade may then be written symbolically as

$$\alpha\vec{V}_A = \alpha\vec{V}_B + \beta\vec{V}_A + \vec{\Omega} \times \vec{R}_{A/B} . \qquad (15)$$

Performing the computations indicated by Eq. 15 and transforming the result into the η,ζ,ξ coordinate system using the transformation of Eq. 5 gives

$$V_A = R\Omega \underbrace{\begin{Bmatrix} \overline{r}c\theta_p - \dot{\overline{\phi}}\{(\overline{a} + \beta_o\overline{r})c\theta_p + \overline{v}\}c\psi - \dot{\overline{\phi}}\{\overline{r}s\theta_p\}s\psi \\ \overline{r}s\theta_p + \dot{\overline{v}} - \dot{\overline{\phi}}\{(\overline{a} + \beta_o\overline{r})s\theta_p\}c\psi + \dot{\overline{\phi}}\{\overline{r}c\theta_p\}s\psi \\ (v'\overline{r} - \overline{v})s\theta_p - \dot{\overline{\phi}}\{\overline{a} + (\overline{v} - v'\overline{r})c\theta_p\}s\psi \end{Bmatrix}_{\eta,\zeta,\xi}} \qquad (16)$$

where the $\dot{}$ dimensionless variables are defined by $\overline{r} = r/R$, $\dot{\overline{\phi}} = \dot{\phi}/\Omega$, $\overline{a} = a/R$, and $\overline{v} = v/R$. In addition, it has been assumed that the order of magnitude for the various terms are as follows:

Order 1 variables: $\overline{r}$

Order $\varepsilon_o^{1/2}$ variables: $\dot{\overline{\phi}}$

Order ε_o variables: $\overline{a}$, β_o, $\overline{v}$, $\dot{\overline{v}}$, v', h/R

In the above velocity equation, terms of order ε_o^2 and higher have been neglected.

The relative velocity of the wind with respect to the moving rotor blade is computed by transforming the wind velocity components into the deformed blade coordinates and subtracting the blade velocity of Eq. 16. This gives

$$\left\{\frac{V_{rel}}{R\Omega}\right\} = \begin{Bmatrix} -\bar{r}c\theta_p - (\bar{V}_r+\delta\bar{V}_r+\delta\bar{V}_y)s\theta_p + c\psi[\delta\bar{V}_x+\phi\bar{V}_r)c\theta_p \\ \quad + \dot{\bar{\phi}}\{(\bar{a}+\beta_o\bar{r})c\theta_p+\bar{v}\}] \\ \quad + s\psi[-(\delta\bar{V}_z-\chi\bar{V}_r)c\theta_p + \dot{\bar{\phi}}\{\bar{r}s\theta_p\} \\ -\bar{r}s\theta_p-\dot{\bar{v}}+(\bar{V}_r+\delta\bar{V}_r+\varepsilon\bar{V}_y)c\theta_p + c\psi[(\delta\bar{V}_x+\phi\bar{V}r)s\theta_p \\ \quad + \dot{\bar{\phi}}\{(\bar{a}+\beta_o\bar{r})\theta_p\}] \\ \quad + s\psi[-(\delta\bar{V}_z-\chi\bar{V}_r)s\theta_p-\dot{\bar{\phi}}\{\bar{r}c\theta_p\}] \\ -(v'\bar{r}-\bar{v})s\theta_p+ c\psi(\delta\bar{V}_z-\chi\bar{V}_r) \\ \quad + s\psi[\delta V_x+\phi V_r+\dot{\bar{\phi}}\{\bar{a}+(\bar{v}-v'\bar{r})c\theta_p\}] \end{Bmatrix}_{\eta,\zeta,\xi} \quad (17)$$

In this equation, terms of order ε_o^2 have been discarded. The order of magnitude assumptions for the wind velocities are as follows:

Order 1 velocities: $\bar{V}_r = (V_h - v_a(r))/R\Omega$
Order ε_o velocities: $\delta\bar{V}_r$, $\delta\bar{V}_x$, $\delta\bar{V}_y$, $\delta\bar{V}_z$

Acceleration Analysis

The acceleration of an arbitrary point P, located at coordinates (η,ζ) within the cross section of the rotor, is given by the usual five-term acceleration equation as

$$\vec{a}_p = \vec{a}_B + \dot{\vec{\Omega}} \times \vec{r}_{P/B} + 2\vec{\Omega} \cdot \vec{V}_P + \vec{\Omega} \times(\vec{\Omega} \times \vec{r}_{P/B}) + \vec{a}_p \,. \quad (18)$$

The various terms in Eq. 18 must all be transformed into the x_p,y_p,z_p coordinate system using the transformation of Eq. 5. The indicated operations of Eq. 18 must be carried out and the results linearized. This tedious activity gives the following expressions for acceleration components in the x_p,y_p,z_p coordinates:

$$\begin{Bmatrix} a_{x_p} \\ a_{y_p} \\ a_{z_p} \end{Bmatrix} = \begin{Bmatrix} -s\theta_p(r\Omega^2\beta_o+2\dot{\phi}\Omega rc\psi+\ddot{\phi}rs\psi+v\Omega^2c\theta_p)-\zeta\Omega^2c\theta_ps\theta_p-\eta\Omega^2c\theta_p^2 \\ c\theta_p(r\Omega^2\beta_o+2\dot{\phi}\Omega rc\psi+\ddot{\phi}rs\psi)-v\Omega^2s\theta_p^2-\zeta\Omega^2s\theta_p^2-\eta\Omega^2s\theta_pc\theta_p+\ddot{v} \\ -r\Omega^2-2\Omega\dot{v}s\theta_p \end{Bmatrix}_{x_p,y_p,z_p} \quad (19)$$

where the above equation retains terms up to order ε_o.

FORCE COMPONENTS

Aerodynamic forces

The lift and drag forces on the airfoil are given by the formulas

$$dL = \frac{1}{2}\rho C_L ch(\xi)W^2d\xi$$

$$dD = \frac{1}{2}\rho C_D ch(\xi)W^2d\xi$$

as shown in Figure 3. However, the force components of interest are given for the structural analysis in the principal inertia axes of the rotor blade, x_p,y_p,z_p or η,ζ,ξ. For the small deformation theory of this analysis there is no difference between these two coordinate systems with respect to the structural equations. The force components of interest are dA_η and dA_ζ which are given by

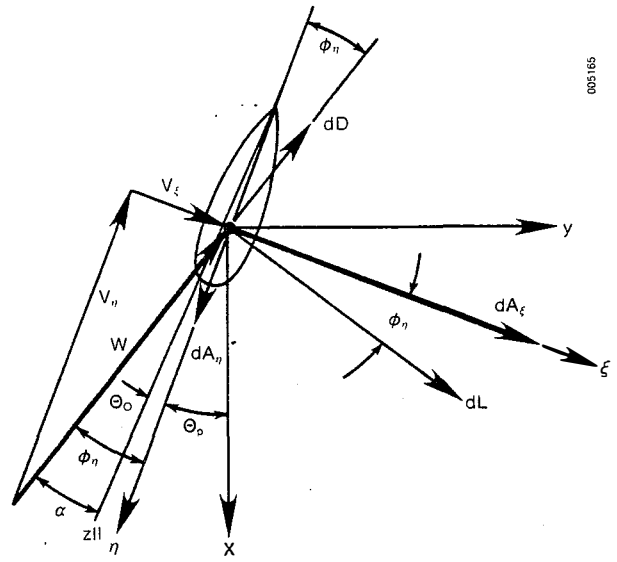

Figure 3. Velocity triangle and coordinate systems used for computation of aerodynamic forces.

$$\begin{Bmatrix} dA_\eta \\ dA_\zeta \end{Bmatrix} = \frac{1}{2}\rho ch(x)Wd\xi \begin{Bmatrix} C_LV_\zeta - C_DV_\eta \\ C_LV_\eta + C_DV_\zeta \end{Bmatrix} \quad (20)$$

where

$C_L(\alpha) = \alpha\, C_{L_\alpha}$ "Lift Coefficient"

$C_D(\alpha) = C_{D_o} + k\, C_L^2$ "Drag Coefficient"

$W = (V_\eta^2 + V_\zeta^2)^{1/2}$

k = constant

$\alpha = \tan^{-1}(V_\zeta/V_\eta) - \theta_o(x)$

$\theta_o(x)$ = The angle between the zero lift line (zLL) and the assumed bending plane. This angle includes the blade pretwist and the offset angle of the airfoil lift curve.

The aerodynamic pitching moment is given by the equation

$$dM_{a.c.} = \frac{1}{2}\rho\, C_{M_{a.c.}}\, ch(\zeta)W^2d\xi \,, \quad (21)$$

where

$C_{M_{a.c.}} = C_{M_{a.c.}}$ (constant) "Pitching Coefficient"

The aerodynamic moment per unit of blade length about the elastic axis, $q^a_{z_p}$, is given by

$$q^a_{z_p} = dM_{a.c.} + dA_\zeta e_{a.c.} \,, \quad (22)$$

where

$e_{a.c.}$ = $(e_{e.a.} - a_c)$ positive if the elastic axis is forward of the aerodynamic center
$e_{e.a.}$ = distance from the leading edge to the elastic axis
a_c = distance from the leading edge to the aerodynamic center.

In the computer code, the lift curve slope C_{L_α} and the drag coefficient C_D may be entered as a function of position along the rotor span, so that reasonable values for lift and drag coefficients are obtained, in regions of relatively large angles of attack.

Inertia Forces

The distributed inertia forces acting along the blade can be computed using Newton's laws as follows

$$d\vec{p}^I = -\vec{a}_p dm = (-\vec{a}_p \rho_b \, d\eta d\zeta) , \qquad (23)$$

where ρ_b is the blade mass density. Then the inertia force per unit length is given by

$$d\vec{p}^I = \iint_{\text{Blade Section}} -\vec{a}_p \rho_b \, d\eta d\zeta . \qquad (24)$$

The inertia moments are computed from the equation

$$d\vec{q}^I = \vec{r}_c \times d\vec{p}^I = -(\vec{r}_c \times \vec{a}_p)\rho_b d\eta d\zeta , \qquad (25)$$

where the vector $\vec{r}_c$ is given as $\{\eta, \zeta, o\}_{\eta,\zeta,\xi}$. Substitution of the acceleration Eq. 19 for $\vec{a}_p$ in Eqs. 24 and 25 gives the inertia forces due to motion of the structure. If the gravitational force is considered as deriving from an acceleration in the X,Y,Z coordinate system it can be treated in a similar manner.

Distributed Forces

The combined loads due to structural motions, gravity, and aerodynamic forces needed to solve the equations of motion are

$$p_{y_p} = dA\zeta + m[-(r\Omega^2\beta_o + 2\Omega\dot{\phi}rc\psi + \ddot{\phi}rs\psi)c\theta_p + v\Omega_p^2 s\theta_p^2 + e_\eta \Omega^2 s\theta_p c\theta_p - \ddot{v}\,] + mg[-\chi c\theta_p + s\theta_p s\psi + \beta_o c\theta_p c\psi] \qquad (26a)$$

$$p_{z_p} = m[r\Omega^2 + 2\dot{v}\Omega s\theta_p] - mgc\psi \qquad (26b)$$

$$q_{x_p} = v'\Omega^2 s\theta_p^2 I^m_{\eta\eta} \qquad (26c)$$

where

$$m = \iint_{\text{Blade Section}} \rho_b d\eta d\zeta = \text{mass/unit length}$$

$$e_\eta = \frac{1}{m} \iint_{\text{Blade Section}} \rho_b \eta \, d\eta d\zeta = \text{Distance along the } x_p \text{ axis to the center of mass, } O(\varepsilon_o)$$

$$I_{\eta\eta} = \iint_{\text{Blade Section}} \rho_b \zeta^2 d\eta d\zeta$$

EQUATIONS OF MOTION AND BLADE LOADS

To develop the flap motion governing equation it is necessary to begin with structural Eqs. 4a and 4d. The tension equation (4d) can be directly integrated to give

$$T(z_p) = \int_{z_p}^{L} m(r\Omega^2 + 2\dot{v}\Omega s\theta_p - gc\psi)dz_p , \qquad (27)$$

where $r \simeq (h + z_p)$.

In order to reduce the flap motion equation to an ordinary differential equation for computer solution, the rotor blade flapping motion is assumed to be of the form

$$v(z_p,t) = \sum_{k=1} s_k(t)\gamma_k(z_p) \text{ where } k = 1 \text{ to } 4 \qquad (28)$$

The flapping displacements are taken in the form of simple polynomials that satisfy the blade kinematic and natural (force) boundary conditions. The time-dependent blade displacements, $s_k(t)$, are determined by numerical integration. For the results presented here only cantilever blade attachment boundary conditions have been considered, but other blade attachments are currently being incorporated into the code.

Substitution of the assumed blade motions given by Eq. 28 into the flap equation, Eq. 4a, gives

$$(-(s_k\gamma_k)''EI_{y_p})'' + (T(s_k\gamma_k'))' + q'_{x_p} + p_{y_p} = 0 , \qquad (29)$$

where a summation over k = 1 to 4 is implied. Now using a Galerkin approach (2) gives

$$\int_o^L \{((-s_k\gamma_k)''EI_{y_p})'' + (T(s_k\gamma_k'))' + q'_{x_p} + p_{y_p}\}\gamma_\ell dz_p = 0 \qquad (30)$$

Integrating by parts and using the boundary conditions required of γ_k leads to an ordinary differential equation in $s_k(t)$, which can be integrated numerically in the time domain.

Carrying out this series of operations, and using the loads q_{x_p} and p_{y_p} from Eqs. 26a-f gives the following expressions for flapping accelerations

$$\ddot{s}_k M_{k\ell} = -s_k K^B_{k\ell} - s_k\{\Omega^2 K^\Omega_{k\ell} + 2\Omega s\theta_p \dot{s}_n K^c_{nk\ell} - c\psi g K^g_{k\ell}\}$$
(Bending) (Tension Stiffening)

$$- c\theta_p\{\Omega^2 + 2\Omega\dot{\phi}c\psi + \ddot{\phi}s\psi\}M^R_\ell$$
(Rigid Body Motion)

$$+ s_k\Omega^2 s\theta_p^2 K^q_{k\ell}$$
(inertia Moment Stiffening)

$$+ \Omega^2 s\,\theta_p c\,\theta_p M^B_\ell + F^a_\ell$$
(Blade Imbalance) (Aero Force)

$$+ s_k\Omega^2 s\theta_p^2 M_{k\ell}$$
(Inertia Force Stiffening)

$$+ g\{-\chi c\theta_p + s\theta_p s\psi + \beta_o c\theta_p c\psi\}M^g_\ell \qquad (31)$$
(Gravity Loads)

where the various coefficients in this acceleration equation are given by

$$M_{k\ell} = \int_o^L m\gamma_K\gamma_\ell dz_p$$

$$M^R_\ell = \int_o^L m(h + z_p)\gamma_\ell dz_p$$

$$M^B_\ell = \int_o^L e_\eta m\gamma_\ell dz_p$$

$$M^g_\ell = \int_o^L m\gamma_\ell dz_p$$

$$K^B_{k\ell} = \int_o^L EI_{y_p}\gamma_k''\gamma_\ell'' dz_p$$

$$K^{\Omega}_{k\ell} = \int_0^L T^{\Omega}(z_p)\gamma_k'\gamma_\ell' dz_p$$

$$K^{q}_{k\ell} = I^{m}_{\eta\eta}(L)\gamma_k'(L)\gamma_\ell'(L) - \int_0^L I^{m}_{\eta\eta}(z_p)\gamma_k'\gamma_\ell' dz_p \quad (32)$$

$$K^{c}_{nk\ell} = \int_0^L T^{c}_{n}(z_p)\gamma_k'\gamma_\ell' dz_p$$

$$F^{a}_{\ell} = \int_0^L dA_\zeta \gamma_\ell dz_p$$

$$T^{\Omega}(z_p) = \int_{z_p}^L m(\xi)(h + \xi)d\xi$$

$$T^{c}_{n}(z_p) = \int_{z_p}^L m(\xi)\gamma_n(\xi)d\xi$$

$$T^{g}(z_p) = \int_{z_p}^L m(\xi)d\xi$$

and all of the above constants are evaluated numerically.

After a steady-state flap solution (trim solution) or after each revolution of a yaw motion solution, the flap displacement, velocity, and acceleration have all been determined and the loads on the rotor can be computed. This is accomplished using the force integration method. The basic structural equations (2a-c) and (3a-c) are numerically integrated along the blade using the loadings due to aerodynamic forces and inertia forces. Additional details on the development of Eq. 31 and the load equation are available in reference (1).

COMPUTER SOLUTION

The computer solution of the equation of motion and the computation of the resulting displacements and loads require a sophisticated interactive program capable of performing a variety of tasks, including input and output of data and results, matrix inversion, time domain analysis, and the computation of spatially dependent blade properties and aerodynamic factors. The nature of the overall project required that the program be flexible, well-documented, and easily modified. The computational requirements of the equation of motion and other associated quantities determined which portions of the program could forego efficiency in favor of flexibility and readability and which portions had to be as efficient as possible.

The computer solution required the creation of two main program sets: Module 1 and Module 2. Module 1 is a data preprocessor. The raw blade and turbine property data file is processed by Module 1 to produce a data file that can be used to solve the equation of motion. It also computes all the coefficient matrices since they are independent of most of the nonturbine-related variables such as wind speed, tower shadow, etc. Module 2 performs the actual model run including solution of the equation of motion, computation of the loads and printing of the results. A flow chart of the program organization is shown in Figure 4.

Solution of the Equation of Motion

The equation of motion for computer solution was given in Eq. 31. The procedure for solving the equation of motion is as follows:

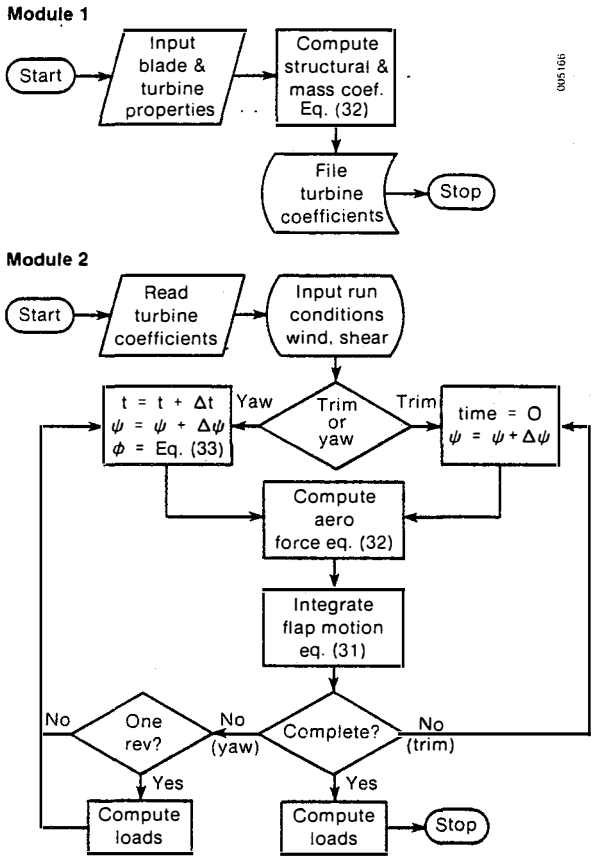

Figure 4. Flow Chart for FLAP Code

1. All the coefficient matrices are multiplied by the inverse of the mass matrix. Thus the mass matrix associated with the blade tip accelerations, when multiplied by its inverse, gives the identity matrix. This results in a set of equations with the blade tip accelerations on one side of the equality and the computed generalized forces on the other side. Multiplication by the inverse mass matrix is only done once at the beginning of Module 2.
2. In this way, the accelerations associated with each flap coordinate function can be evaluated numerically by substituting the current values for the flap velocities and displacements into the force side of the equation.
3. The blade tip displacements are computed by solving the second-order differential equation relating acceleration, velocity, and displacement. The solution is performed via the modified Euler predictor-corrector method, which uses the current blade tip accelerations and the previous values of the displacements and velocities.
4. The blade loads are computed only at the completion of a trim solution (steady-state) run.
5. The solution during time-dependent prescribed yawing motions is run at the completion of the trim solution. Loads are computed at the completion of each revolution during the yawing solution. Yaw motion is prescribed according to the simple equation

$$\phi(t) = \phi_o + \phi_a \sin(\omega_\phi t) \qquad (33)$$

where ϕ_o is the initial yaw angle, ϕ_a is the amplitude of the motion, and ω_ϕ is the frequency of the motion.

Loads Output

A set of nine blade motion and blade load values is computed for each spanwise location on the blade (generally 11) and each azimuth position (usually 36). The nine quantities that are output in tabular form are

1. Blade Section Flap Displacement (ft)
2. Blade Section Flapwise Slope (ft/ft)
3. Blade Section Flap Velocity (ft/sec)
4. Blade Tension (lb)
5. Blade Edgewise Shear (lb)
6. Blade Flapwise Shear (lb)
7. Blade Flapwise Moment (lb-ft)
8. Blade Edgewise Moment (lb-ft)
9. Blade Torsion (lb-ft)

COMPARISON OF RESULTS WITH TEST DATA

Turbine Model

The turbine modeled was a three-bladed, downwind system with a rotor diameter of 33 ft. The rotor rotation speed was 72 rpm and the blade first natural frequency was about 3.95 hz, or about 3.3 times the rotor passage frequency. The blade has a constant chord of 18 in., no twist, and is coned at 3.5°.

Structural and mass properties for the rotor blade were obtained from the basic design information provided by the manufacturer to Rocky Flats, and from reference (3). However, it required a careful review of this material and some judgment to extract the necessary information.

The blade aerodynamic properties were modeled using Princeton University data for the lift and drag coefficients as specified in reference (4). For the current version of the FLAP code the lift curve is modeled as a straight line; however, the slope of this straight line is varied as a function of blade span position in order to get a reasonable approximation for the lift coefficient. For this modified 654-421 airfoil the lift curve is quite nonlinear. For the three cases run during this study the angle of attack was between 0° and 15° over 75% of the blade.

The tower shadow deficit was assumed to be approximately 25% to 30%, over a pie-shaped section of about 25 to 30° as indicated by the data given in reference (5). The 350-ft meteorological tower at Rocky Flats indicates that wind shear coefficients are typically between 0.1 to 0.25. This range of values was used for the study.

Experimental Data

For this comparison, data for three specific wind speed cases were analyzed: 12 mph, 18 mph, and 20 mph. For each wind speed the flap bending moment at 20% blade span was used for comparison. The comparison was made using the banding moment at this location averaged over 20 rotor revolutions. This azimuth-averaged bending moment was computed by averaging the bending moment data at 33 azimuth locations around the blade circle of travel. All of the data were manually digitized from analog visicorder traces. For comparison of cyclic responses which are of primary interest the mean bending moment has been subtracted.

The data were azimuth averaged in this manner to average out the random wind inputs for comparison with the code predictions which are deterministic. The desired comparison is for the response of the blade to gravitational loading, tower shadow effects, and average wind shear effects. The azimuth averaging process should clarify these effects.

Discussion of Results

The FLAP code was run several times for the 18-mph wind speed case to determine sensitivity to tower shadow configuration and wind shear exponent. The results of this sensitivity study are illustrated in Figure 5, which is a plot of the blade cyclic

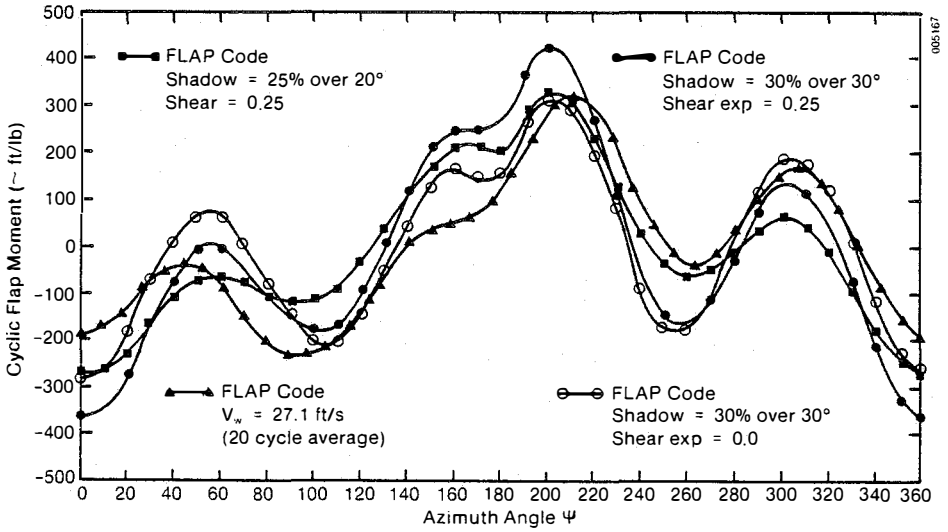

Figure 5. Sensitivity of predicted flap moment at 20% span to the tower shadow and wind shear parameters.

moment at 20% span versus azimuth angle. Also plotted in the figure are the experimental data for this case. The most notable difference is in the tower shadow region, where the predicted results are significantly above the experimental measurements.

The most likely cause for this deviation is the pie-shaped tower shadow used in the computer model. The actual shadow region is rectangular in shape, and the shadow effect is felt fairly gradually over a much wider region than is predicted by the computer model. In other respects the prediction is very similar in character to the experimental measurements. By comparing the various cases run, the general influence of changing the shadow and shear exponent can be judged. However, because the changes in harmonic content are subtle, a general cause and effect relationship is difficult to see. A qualitative "best match" prediction was obtained by including 10^{o} of yaw. This case is shown in Figure 6. Using these same numerical values for tower shadow (25% deficit over a 30^{o} sector), with a wind shear exponent of 1/7 and a 10^{o} yaw angle, the FLAP predicted bending moment is compared with experimental data at wind speeds of 12 mph and 20 mph in Figures 7 and 8 respectively. As can be seen the comparison is quite favorable. The reader wishing more details concerning the experimental work and the comparison with other predictive codes is referred to Wright (6).

The reader is cautioned that a validation study using only one turbine configuration does not prove the code is valid for all situations. The comparison results in this case were for a turbine with a relatively stiff blade. The flapping motions were small and neither control system effects nor tower motion effects were significant. Until the FLAP code is verified against other more flexible rotor systems it cannot be considered a validated computation procedure.

ACKNOWLEDGMENT

This research work was supported by the U.S. Department of Energy, Federal Wind Energy Program through the Energy Systems Group of Rockwell International Corporation, Rocky Flats Plant, Golden, CO 80401.

REFERENCES

1. Thresher, R. W. and Hershberg, E. L., "Computer Analysis of Wind Turbine Blade Static and Dynamic Loads," RFP-76824, March 1984, prepared by Oregon State University for Rocky Flats Plant, Wind Systems program.

2. Dym, C. L. and Shames, I. H., Solid Mechanics: A Variational Approach, McGraw Hill, 1973, pp. 164-176.

3. Adler, F. M., et al., "Development of an 8kW Wind Turbine Generator for Residential Type Applications, Phase I - Design and Analysis," Grumman Energy Systems, Inc., Volume II Technical Report, RFP-3007-2, March 1980.

4. Sweeney, T. E. and Nixon, W. B., "Two-Dimensional Lift and Drag Characteristics of Grumman Windmill Blade Section," Informal Report, Princeton University, Feb. 1978.

5. Snyder, M. H. and Wentz, W. H. Jr., "Dynamics of Wakes Downstream of Wind Turbine Towers," Conference Proceedings, Wind Turbine Dynamics, NASA Conference Publication 2185, pp. 363-373, Feb. 1981.

6. Wright, A. D., et al., "Wind Turbine Rotor Loads--Comparison of Measured and Calculated," Proceedings of the NASA Wind Turbine Workshop, Cleveland, Ohio, May 1984.

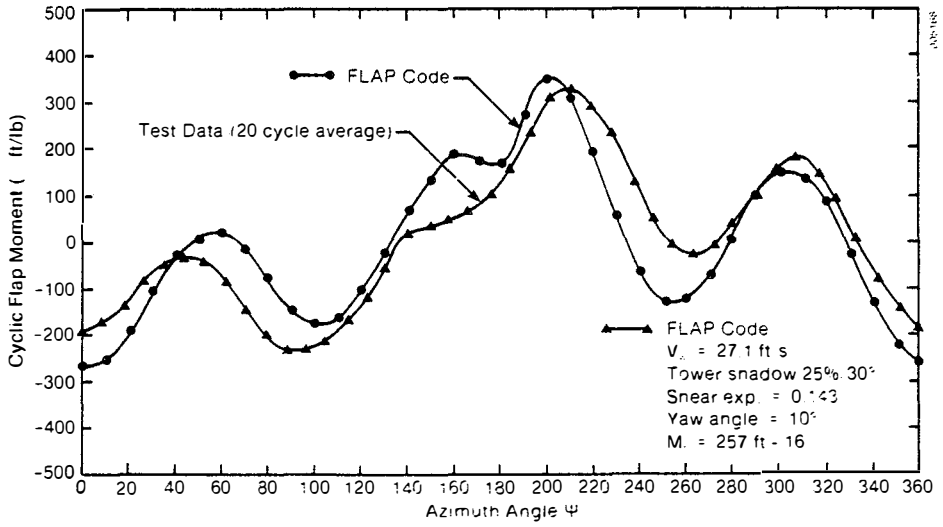

Figure 6. Best prediction of flap moment at 20% span at 18 mph.

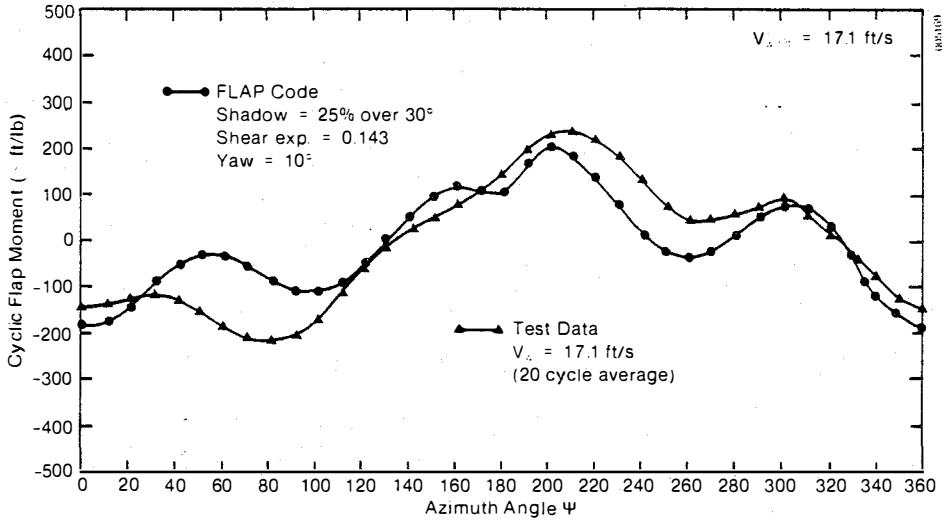

Figure 7. Comparison of predicted flap moment at 20% span at 12 mph.

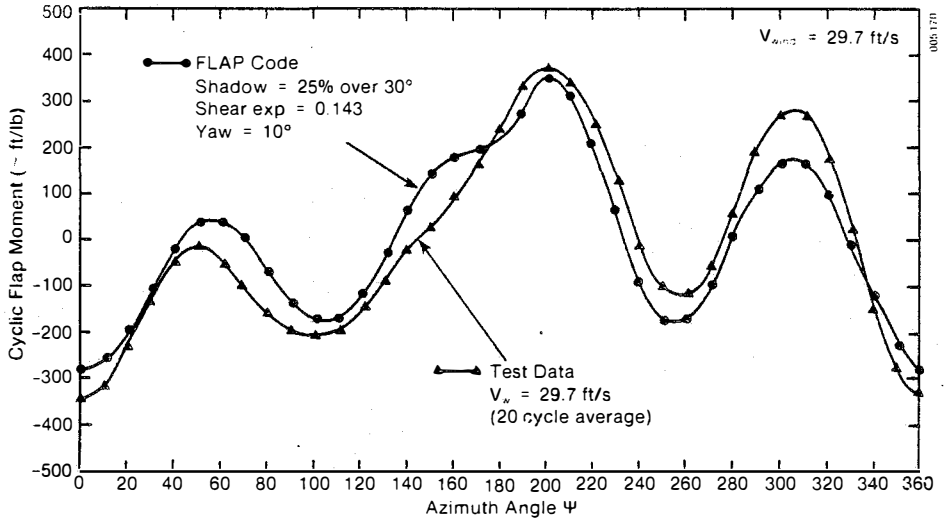

Figure 8. Comparison of predicted flap moment at 20% span at 20 mph.